Supporting Information for
Original article

ZDHHC12-mediated claudin-3 *S*-palmitoylation determines ovarian cancer progression

Meng Yuan[a,†], Xiaobing Chen[a,†], Yitang Sun[c], Li Jiang[a], Zhongni Xia[d], Kaixiong Ye[c], Hong Jiang[b], Bo Yang[a], Meidan Ying[a], Ji Cao[a,*], Qiaojun He[a,*]

[a]*Zhejiang Province Key Laboratory of Anti-Cancer Drug Research, College of Pharmaceutical Sciences, Zhejiang University, Hangzhou 310058, China*

[b]*Interdisciplinary Research Center on Biology and Chemistry, Shanghai Institute of Organic Chemistry, Chinese Academy of Sciences, Shanghai 100098, China*

[c]*Department of Genetics, University of Georgia, Athens, GA 30602, USA*

[d]*Tongde Hospital of Zhejiang Province, Hangzhou 310012, China*

Received 30 December 2019; received in revised from 18 February 2020; accepted 27 February 2020

[*]Corresponding authors.

E-mail addresses: caoji88@zju.edu.cn (Ji Cao), qiaojunhe@zju.edu.cn (Qiaojun He).

[†]These authors made equal contributions to this work.

Supplementary figure 1

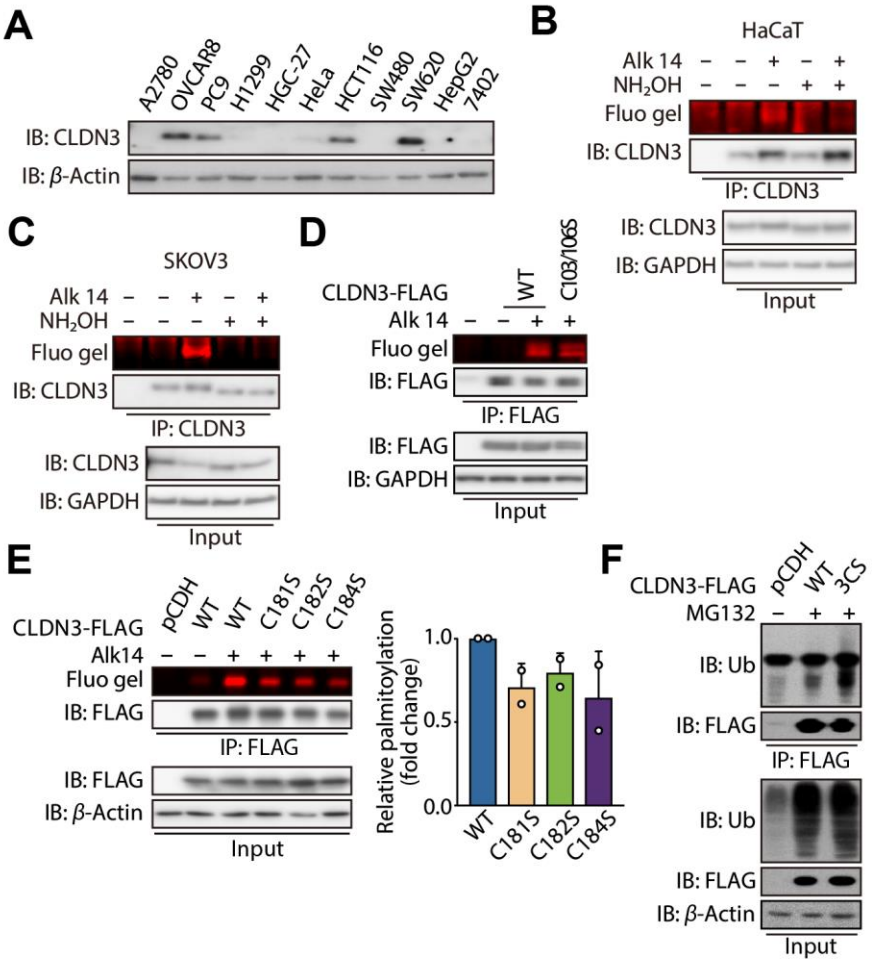

Figure S1 (A) Protein expression level of CLDN3 in different types of cancer cell lines were analyzed by immunoblotting. (B) In-gel fluorescence shows the *S*-palmitoylation level of endogenous CLDN3 in HaCaT cells. (C) In-gel fluorescence shows the *S*-palmitoylation level of endogenous CLDN3 in SKOV3 cells. (D) In-gel fluorescence shows the *S*-palmitoylation level of FLAG-tagged CLDN3 C103/106S compared to CLDN3 WT. FLAG-tagged CLDN3 C103/106S or WT was transfected in 293T cells for 24 h before submitted to immunoprecipitation and SDS-PAGE. No change in fluorescence intensity indicated that no *S*-palmitoylation occurs at these two cysteine sites. (E) In-gel fluorescence shows the *S*-palmitoylation level of CLDN3 with single cysteine residue mutants. Right histogram shows the quantification of the fluorescence intensity relative to that of CLDN3 WT. Values with error bars indicate mean ± SD of two independent replicates. (F) The endogenous ubiquitin levels of CLDN3 WT and CLDN3 3CS were detected by Western blot after co-immunoprecipitation. Overexpressing FLAG-tagged CLDN3 WT or CLDN3 CS 293T cells were lysed by 4% SDS buffer after treatment of MG132 for 6 h. Cell lysate was submitted to anti-FLAG immunoprecipitation and immunoblotting. The ubiquitination level of CLDN3 3CS was higher than CLDN3 WT, suggesting the less stability of CLDN3 3CS.

Supplementary figure 2

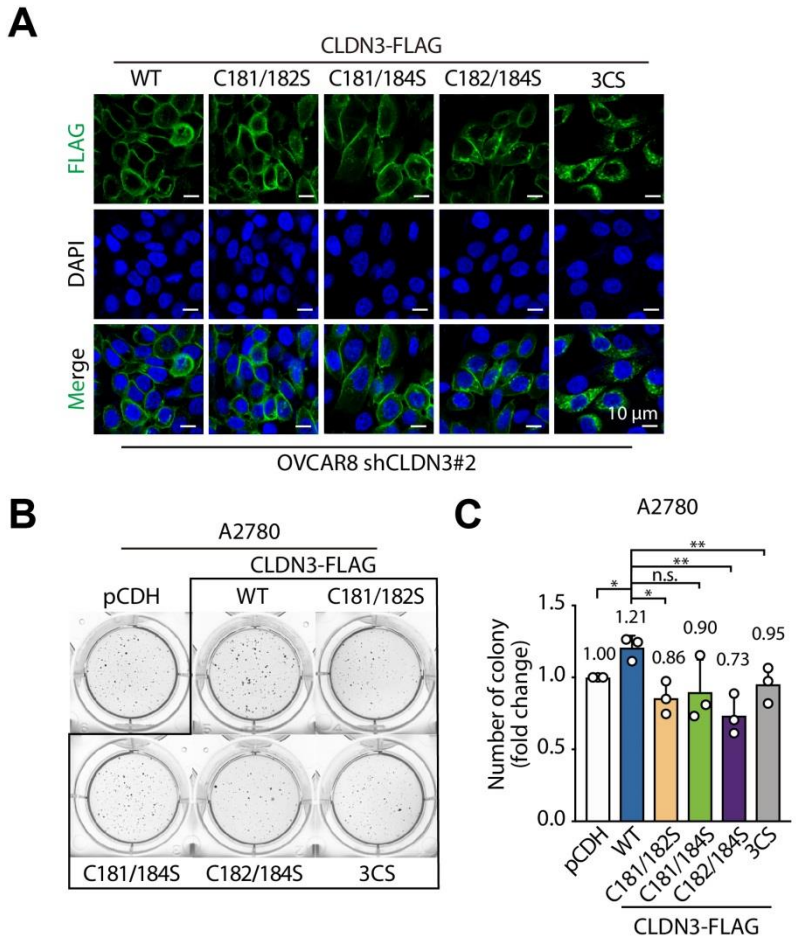

Figure S2 (A) Confocal images show the intercellular localization of FLAG-tagged CLDN3 WT and mutants stably expressing in shCLDN3 OVCAR8 cells. Cells expressing FLAG-tagged CLDN3 3CS were treated with MG132 for 4 h before fixed and immunofluorescence staining with indicated antibodies. (B) Representative data from soft agar colony formation assay of A2780 cells expressing FLAG-tagged CLDN3 WT or mutants. 1.5×10^3 cells were cultured in DMEM medium contained 10% FBS and 0.35% agarose gel for 21 days. Cell colonies were stained by MTT. (C) The quantification of the colony numbers in soft agar colony formation assay (B). Values with error bars indicate mean ± SD of three independent replicates (n.s. indicates no statistic difference; $^{*}P < 0.05$; $^{**}P < 0.01$).

Supplementary figure 3

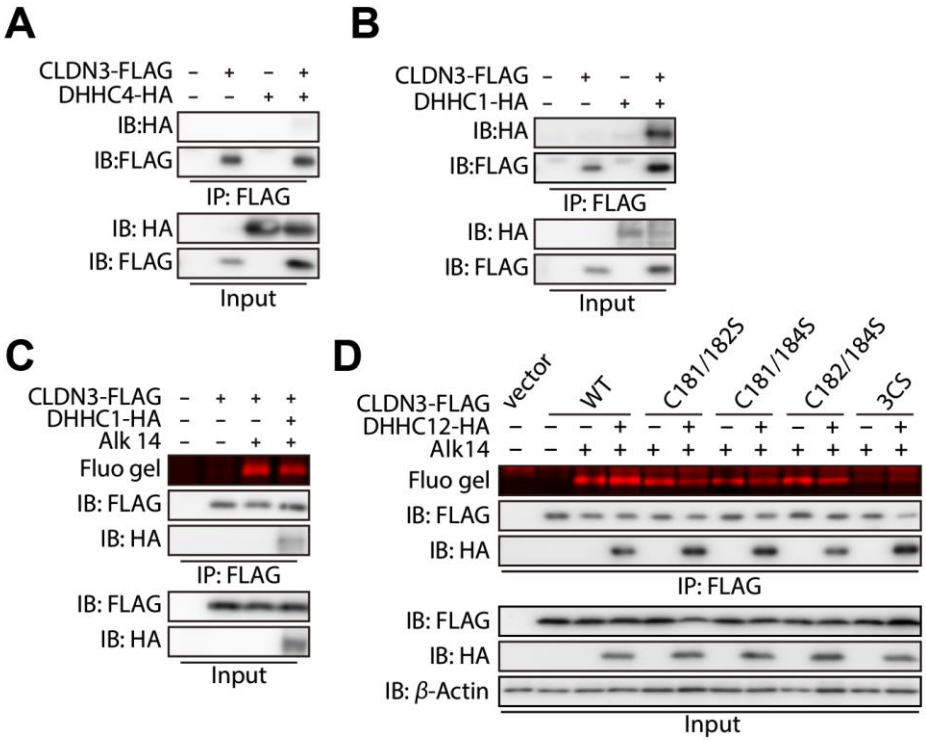

Figure S3 (A) Identification of the interaction between HA-tagged DHHC4 and FLAG-tagged CLDN3 by co-immunoprecipitation with anti-FLAG antibody. No significate interaction between DHHC4 and CLDN3 was determined by immunoblotting. (B) and (C) Identification of the interaction between HA-tagged DHHC1 and FLAG-tagged CLDN3. The expression of DHHC1 and CLDN3 failed to affect the *S*-palmitoylation level of CLDN3. (D) In-gel fluorescence shows the *S*-palmitoylation level of wild type CLDN3, double cysteine mutants and triple cysteine mutants effected by co-expressing DHHC12 in 293T cells. The overexpression of DHHC12 had no effect on the *S*-palmitoylation intensity of each CLDN3 mutants while it enhanced the *S*-palmitoylation intensity of CLDN3 WT.

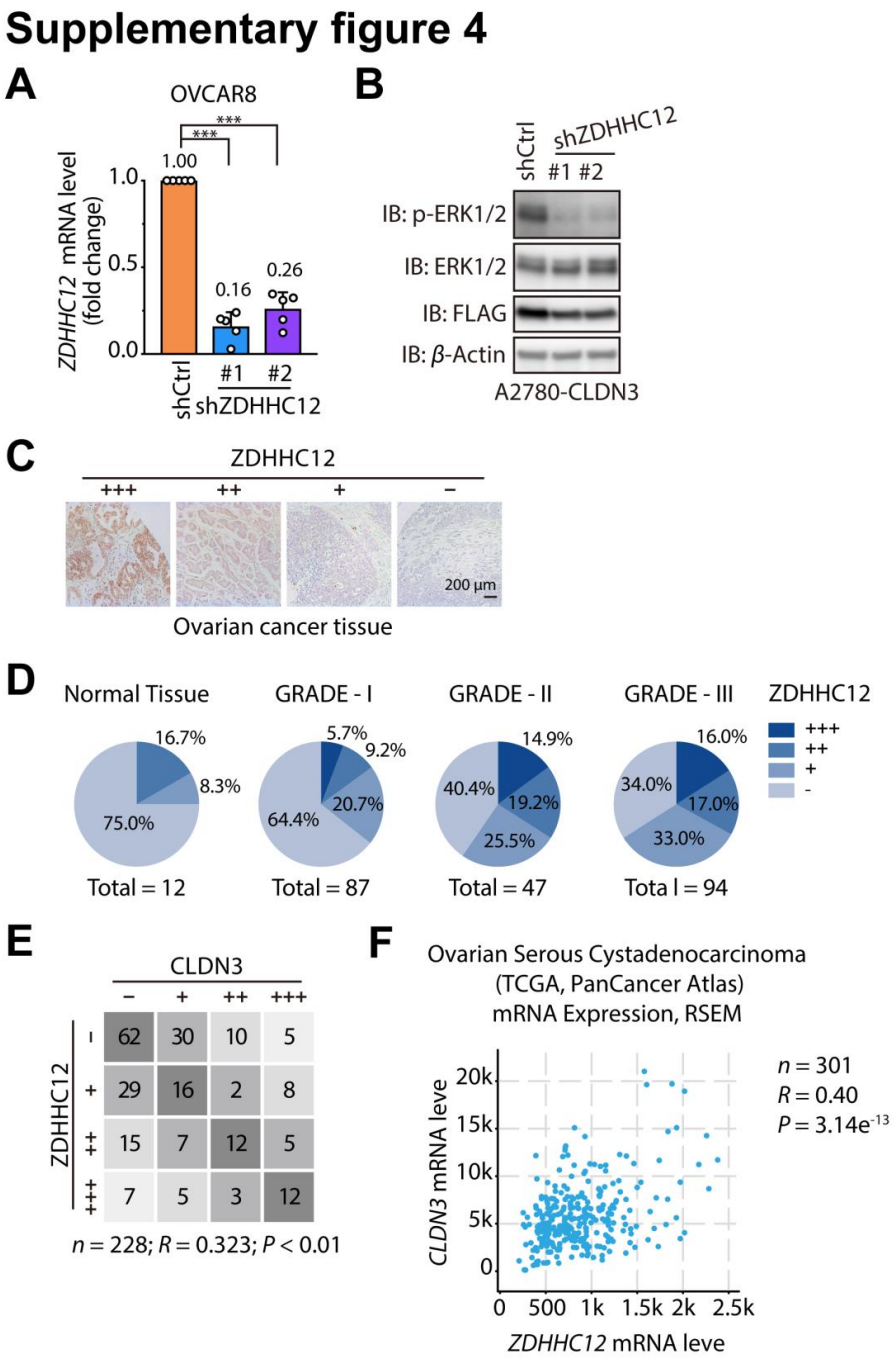

Figure 4 (A) The knockdown efficiency of shRNA against ZDHHC12 in OVCAR8 cells validated by real-time PCR. Values with error bars indicated means ± SD of five independent replicates ($^{***}P < 0.001$). (B) Downregulation of phosphorylated ERK1/2 in shZDHHC12 A2780 cells, compared to shCtrl group, was indicated by immunoblotting. Cell lysates were harvested in 5 days after lentivirus infection (MOI = 2), followed by SDS-PAGE and immunoblotting with indicated antibody. (C) Representative images of different score of immunohistochemical stain, indicating different expression level of ZDHHC12 (+++ indicates high expression; ++ indicates median expression; + indicates low expression; – indicates negative expression). (D)

The pie chart shows the proportion of different expression level of ZDHHC12 in each ovarian tumor grade (from GRADE-I to GARDE-III and normal tissue group). Darker shades of blue indicate higher expression of CLDN3 (n = 240). (E) The correlation analysis between of CLDN3 and ZDHHC12 expression level based on samples in human ovarian cancer tissue arrays (12 normal tissue samples were excluded). Correlation coefficient was described as Pearson correlation coefficient that analyzed by Graph Prims 7.0 software. Darker shades of gray indicate higher positive correlation (n = 228; R = 0.323; R, Pearson correlation coefficient). (F) The scatter plot shows the relationship of *ZDHHC12* and *CLDN3* mRNA level in samples from ovarian serous cystadenocarcinoma (TCAG, PanCancer Atlas, https://www.cbioportal.org). Pearson correlation coefficient was determined to describe the correlation of ZDHHC12 and CLDN3 in selected database. Batch normalized from Illumina HiSeq_RNASeqV2. (n = 301; R = 0.40; P = 3.14e^{-13}).

Table S1 Sequence of shRNA.

Gene	Forward prime	Reverse prime
CLDN3#1	CCGGAGAAGTACACGGCCA CCAAGGCTCGAGCCTTGGTG GCCGTGTACTTCTTTTTTG	AATTCAAAAAAGAAGTACAC GGCCACCAAGGCTCGAGCCTT GGTGGCCGTGTACTTCT
CLDN3#2	CCGGGGTGACCGCCAATACT TGACCCTCGAGGGTCAAGTA TTGGCGGTCACCTTTTTG	AATTCAAAAAGGTGACCGCC AATACTTGACCCTCGAGGGTC AAGTATTGGCGGTCACC
ZDHHC12#1	CCGGATGGACCCTGGCTACG TGAATCTCGAGATTCACGTA GCCAGGGTCCATTTTTTG	AATTCAAAAAATGGACCCTG GCTACGTGAATCTCGAGATTC ACGTAGCCAGGGTCCAT
ZDHHC12#2	CCGGGCTACCGTCTTGTGCC TGAAACTCGAGTTTCAGGCA CAAGACGGTAGCTTTTTG	AATTCAAAAAGCTACCGTCTT GTGCCTGAAACTCGAGTTTCA GGCACAAGACGGTAGC

Table S2 Sequence of real-time PCR.

Gene	Forward prime	Reverse prime
β-Actin	ATTCCTATGTGGGCGACGA G	CCAGATTTTCTCCATGTCGTC C
zDHHC12	CTGGTAGCCAGGAACACGA C	CCACAGAAAAAGTGGGCCAG

Table S3 The value of hazard ration of 23 claudins in different types of cancer.

Gene	Bladder			Breast		Colon		Ovarian			Liver
	TCGA	GSE 31684	GSE 48276	TCGA	GSE 21653	GSE 41258	GSE 39582	GSE8 842	GSE 63885	TCGA	TCGA
CLDN1	0.92	1.05	1.04	1.09	1.18	0.97	1.06	2.61	1.41	1	0.99
CLDN2	1	1.22	1.08	1.15	1.51		0.97	0.65	1.16		0.99
CLDN3	0.98	0.85	0.99	1.04	0.96	1.02	0.86	30.01	1.04	0.92	0.99
CLDN4	0.93	0.87	0.93	1.12	0.94	1.22	0.88	1.13	1.04	1.07	1.05
CLDN5	1.27	1.06	0.77	1.43	0.64	1.55	1.14		1.44	0.96	0.94
CLDN6		0.84	0.92	1.15	1.77	3.24	1.07		1.56	0.89	1
CLDN7	0.92	0.89	0.83	1.01	0.9	0.85	0.77		1.27	0.91	1
CLDN8		1.24	0.96	1.04	1.09	1.05	0.94		1.05	1.23	
CLDN9	0.99	1.16	1.01	1.62	2.07	3.05	1.33	0.84	0.84	1.04	1
CLDN10		1.35	0.79	1.14	1.06	0.8	0.92	1.36	0.56	0.97	1.02
CLDN11	1	1.18	1.03	1.47	0.9	2.03	1.2	0.57		1.58	1.06
CLDN12	0.98	1.47	1.16	0.96	0.83		0.77		0.37		1.11
CLDN14	0.9	2.48	1.02	0.87	2.1	0.49	0.82	1.7	1.07		0.92
CLDN15	1.03	1	1.11	1.34	1.02	0.89	0.87	2.81		1.14	0.87
CLDN16		2.08	1.16	1.29	1.33	0.57	1.23		2.45	0.92	1
CLDN17		1.82	0.63	0.73	0.92	1.71	0.86		1.65	1	
CLDN18		1.15	1	0.71	5.21	1.82	0.92		0.8	1.12	1.02
CLDN19		1.08	1.07	1.07	2.92		0.82			0.66	1.01
CLDN20		1.39	0.66		1.98		1.82				
CLDN21									0.84		
CLDN22		1.04				2.78					
CLDN23	0.86	0.88	1.02	1.09	1.19		0.89				

Table S3 The value of hazard ration of 23 claudins in different types of cancer (continue).

Gene	Stomach	Lung			Prostate	Pancreatic	Cervical	Mesothelioma	Sarcoma	Kidney
	TCGA	TCGA	GSE 42127	GSE 3141	TCGA	TCGA	TCGA	TCGA	TCGA	TCGA
CLDN1	0.98	0.91	1.08	0.92	1.59	1.48	0.95	1.05	1.08	1.04
CLDN2	0.96	0.86	0.95	0.94	1.08	1.08	1.02	1.02	1.01	0.93
CLDN3	1	0.55	0.99	0.99	1.09	0.91	0.97	1.02	1.02	0.96
CLDN4	1.01	0.56	0.92	1.04	1.15	1.27	0.95	1.09	0.98	0.67
CLDN5	0.64	1.3	0.84	0.9	0.95	0.77	0.88	1.12	0.94	0.93
CLDN6	1.23	1.12	1.12	1.07	0.97	1	1.02	1.08	1	1.03
CLDN7	1.01	0.24	0.98	1	2.49	1.21	1	1.03	1.03	0.96
CLDN8		0.86	1.1	0.88	1.54	1.02	0.98			1
CLDN9	0.04	1.33	0.95	1.28	1.5	0.93	1.8	1.01	1.01	1.1
CLDN10	0.26	0.81	1.09	1.03	0.94	0.81	0.99	1.01	1.01	0.95
CLDN11	0.24	1.08	1.03	1.1	1.15	0.99	1	1.01	1.02	1.26
CLDN12	1	0.9	1.09	1.18	0.55	1.19	1.8	0.93	0.94	0.73
CLDN14	2	1.54	0.98	1.03	1.33	1.19	0.98	1.05	1.02	1.23
CLDN15	1	1.03	0.89	0.89	1.85	0.66	1.05	0.8	0.81	1.44
CLDN16	0.23	0.86	1.08	1.05	1.2	1.1	1	1.01		1.01
CLDN17	0	1.93	1.45	0.98						0.99
CLDN18	1	0.94	0.9	0.88	1.01	1.05	1.02	1.05	1.01	1.03
CLDN19	0	0.37	0.92	1.1	1.07	0.99	0.99			1
CLDN20	0.03	0.9	1.07	0.88	0.98	0.99	1.01	0.98	1	1
CLDN21										
CLDN22	5.27	1.98	1.15	0.96						1.02
CLDN23		1.16	0.88	1.26	0.5	1.15	1.07	0.9	0.81	0.85